

# Effect of Nano Size TiO<sub>2</sub> Particles on Mechanical Properties of AWS E 11018M Type Electrode

Tapan Kumar Pal, Utpal Kumar Maity

Welding Technology Centre, Metallurgical and Material Engineering Department, Jadavpur University, Kolkata, India.  
Email: tkpal.ju@gmail.com

Received February 21<sup>st</sup>, 2011; revised May 16<sup>th</sup>, 2011; accepted July 1<sup>st</sup>, 2011.

## ABSTRACT

Addition of nano size particles of TiO<sub>2</sub> in the coating of shielded metal arc welding electrode (E 11018M) partially substituting the conventional micro size TiO<sub>2</sub> was studied for possible enhanced electrode characteristics. The results show that the nano size particle of TiO<sub>2</sub> improved recovery of elements such as Mn, Ni, Mo, Ti etc. as well as increased all-weld-metal tensile and charpy impact properties at -51 °C. Furthermore, the charpy impact properties were found to be very sensitive to variations in Ti content of the weld deposit.

**Keywords:** High Strength Steel, Coated Electrode, Nano Size TiO<sub>2</sub>, Strength and Toughness

## 1. Introduction

High strength steels are increasingly employed in many applications due to the advantage they offer such as size and weight reduction along with greater load bearing capacities [1]. Increased use of high strength structural steels poses a need for adequate welding consumable for such materials. This leads to a significant advance in electrode formulation to obtain weld deposits with high values for strength and good toughness [2]. Structural safety in welded joints are obtained by imposing requirement on toughness by setting charpy V-notch levels at the lowest design temperature [3]. The achievement of adequate toughness value increasingly difficult as the weld metal tensile strength increases. It has been well established that maintaining good toughness become more problematic as strength increases above in the region of 690 Mpa [1,4]. One way to obtain improved weld metal toughness is through micro structural control, which requires taking into account the weld metal chemistry.

Steel manufacturers have addressed the challenges of increasing toughness in steel through grain refinement, precipitating hardening, solid solution hardening, thermo mechanical treatment and the promotion of low temperature transformation products such as martensite and bainite. Since weld metals are not usually given any thermo mechanical or special heat treatment, many research works have carried out by varying elemental compositions or welding parameters with the aim of op-

timizing weld metal properties [5-7]. For the weld metal of 780 MPa or lower strength steel, the effect of microstructure and oxygen content has been clearly demonstrated. Acicular ferrite is an ideal microstructure for these weld metals, and the increase in the amount of acicular ferrite leads to improvement both in strength and toughness [8,9]. The prior austenite grain size, inclusion and specific alloying addition that hinder grain boundary ferrite nucleation all are important consideration in achieving optimum weld metal acicular ferrite and properties [10].

Weld consumables generally contain a small amount of Ti to achieve stabilized transfer of molten droplets during arc welding and it had been well known that Ti bearing weld metal is preferably refined. Watanabe *et al.* [11] experimentally changed oxygen contents in Ti bearing gas metal arc weld metals and found that Ti oxides effectively nucleate fine intragranular acicular ferrite. Mori *et al.* [12] also proposed that oxide particles having surface coating of TiO or those particles which are wholly TiO would be the most potent site for nucleation of acicular ferrite since disregistry between TiO and ferrite is only three percent.

In the present investigation, a novel approach has been attempted to develop AWS E11018M electrode. The study consisted of an addition of nano size particles of TiO<sub>2</sub> to the coating of shielded metal arc welding electrode (E11018M) partially substituting the original (micro size) TiO<sub>2</sub> and the effect of such addition on micro-

structure and mechanical properties of all-weld metal.

## 2. Experimental

### 2.1. Preparation Coated Electrode

The AWS E11018M is a basic coated high strength steel electrode. The core wire used for electrode was non-rimming (semi killed) electrode quality steel of 3.15 mm diameter and 450 mm length with a nominal composition of C = 0.05%, Mn = 0.48%, Si = 0.018%, S = 0.018%, P = 0.022%. The composition of the flux ingredients for E11018 M was kept constant as given in **Table 1**, except the micro size TiO<sub>2</sub> particles which were partially replaced with nano size TiO<sub>2</sub> particles. In the present investigation, out of 1.5% micro size TiO<sub>2</sub> particles in total flux ingredient, 1/3rd (33.33%) of it was replaced by the nano size TiO<sub>2</sub> particles for experimentation.

Hydraulic electrode extrusion machine was used to produce the experimental electrodes of size 4mm. No apparent effect was observed with nano size TiO<sub>2</sub> particles on the extrusion behavior of the electrodes. The flux coating has sufficient green strength and having smooth appearance. The electrodes were dried in the oven to the following sequence: at room temperature for 24 hours, at 60°C for 30 min, at 90°C for 10 min., at 120°C for 15 min., at 200°C for 5 min., at 300°C for 5 min. and finally at 420°C for 50 min.

### 2.2. All-Weld—Metal Test Coupons

Four different all-weld metal samples were made with electrodes having two without nano size TiO<sub>2</sub> particles *i.e.* MMAW-I and MMAW-II and two with nano size TiO<sub>2</sub> particles *i.e.* MMAWN-I and MMAWN-II in flat position according to ISO 2560-73. Welds were deposited on a groove of carbon steel (ASTM A131 grade B) plate of 16 mm thick using the different developed electrodes. The groove design is shown in **Figure 1**. The welding parameters as given in **Table 2** were used as per AWS A 5.5 - 1996. The electrode was inclined approximately at 50° - 60° along the welding direction using DC (+). Sixteen no.s of passes in eight layers were required to

**Table 1. Composition of flux ingredients used for coating in E11018M type electrode.**

Flux constituent	Wt %
Limestone	30.45
Fluorspar	22.75
Iron Powder	22.50
Ferro alloys	15.05
Other Minerals	6.25
Extrusion Agents	1.50
TiO <sub>2</sub>	1.50

Note: Liquid silicates used (for 1000 gm flux ingredients powder): Potassium silicate = 130 gm, Sodium silicate = 55gm and Water = 10 gm.

**Table 2. Welding parameters used.**

Current type	DC (+)
Welding current	126 amp.
Open circuit voltage	76 volt.
Welding voltage	22 volt.
Welding speed	90 mm./minute
Inter-pass temperature	100°C

completely fill up the groove of an experimental weld test block.

### 2.3. Test Weld Block and Location of Test Specimen

From each test weld block, all-weld tensile specimens, transverse V-notch charpy impact specimens and metallographic specimens were extracted. The location for each type of specimen is shown in **Figure 2**.

### 2.4. Metallographic Study

Specimens for metallographic analysis from the weld metal cross section, perpendicular to the welding direction, were cut, ground and polished by standard methods. They were then etched with 2% nital and examined under optical microscope and scanning electron microscope (SEM).

### 2.5. Tensile Testing

All-weld tensile specimens were machined longitudinally from the weld deposits with dimension as per AWS A 5.5-1996. The tensile tests were carried out in a Servo-

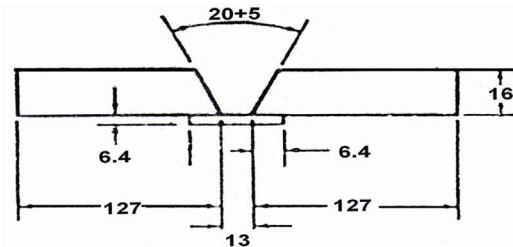


**Figure 1. Groove design.**

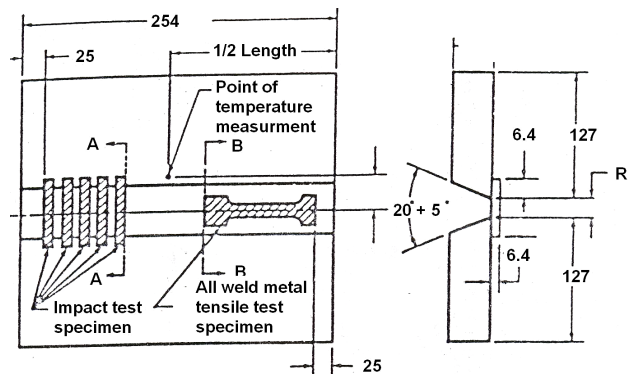


**Figure 2. Test weld block and location of the test specimens.**

Electric (Instron 8862) type 100 kN capacity universal testing machine at a cross head speed of 0.5 mm/min. Tensile test data such as YS, UTS and % elongation was recorded for each all-weld sample. For each electrode three samples were tested and average of three samples was reported.

## 2.6. Vickers Hardness Testing

Hardness test was performed on metallography samples using Vicker's hardness testing m/c with a square based diamond pyramid indenter having an included angle of 136° under a load of 30 kg.

## 2.7. Charpy Impact Testing and Fracture Surface Study

For charpy impact testing, standard 55 × 10 × 10 × mm size transverse specimens were machined and notch was kept in weld metal perpendicular to the weld direction. Charpy impact specimens were tested at -51°C which was achieved by adding acetone in liquid nitrogen. The temperature was measured with electronic thermometer. For each electrode five samples were tested and average of five samples was reported. The broken charpy impact specimens were examined under Scanning Electron Microscope to understand fracture micro-mechanism.

## 3. Results and Discussion

### 3.1. Chemical Composition of Weld Deposits

The chemical composition of different weld deposits is given in **Table 3**. The final weld metal chemical composition is determined by the slag-metal reactions that occur in the weld pool [13-15]. Research into slag-metal reactions has generally been done within the limited scope of a single flux system. However, the complexity of the welding environment as well as the nonideal behaviour of the reactions that occur in the arc, lead to too many variables, which make accurate prediction of the effect of specific changes in system parameters difficult. Even small changes in the flux coating can result in large

variations in the behaviour of the flux system, which in turn leads to large variations in the metallurgical processes occurring in the weld pool.

Although chemical equilibrium is not achieved in a weld pool, a trend toward equilibrium is generally observed that can be estimated using fundamental thermodynamic principles. Oxidation reactions in the weld pool can be described by the following generic reaction:



According to the law of Mass Action, the equilibrium constant,  $k$ , for Equation (1) can be written as follows:

$$k = \frac{[a_{M_xO_y}]}{[a_M]^x [a_O]^y} \quad (2)$$

where,  $[a_M]$  and  $[a_O]$  are the activities of the weld metal alloying element, M and oxygen, respectively, and  $[a_{M_xO_y}]$  is the activity of the metal-oxide inclusion in the weld metal. For equilibrium considerations, the activity of the metal-oxide can be taken as unity, which leads to the following relation:

$$k = \frac{1}{[a_M]^x [a_O]^y} \quad (3)$$

With knowledge of the oxidation reactions that will occur in the solidified weld pool, it is possible to predict the direction toward which these reactions will go as changes are made in the welding flux.

Competing chemical reactions within the weld pool will also affect the final weld metal chemical compositions. As local concentrations of alloy elements vary with solidification [16,17], the local activity of the alloying elements will change, altering the amount of alloying additions that will be oxidized. As a result, these competitive reactions will alter the predicted weld metal chemical composition.

Results of all-weld metal chemical composition as presented in **Table 3** demonstrate that the recovery of the

**Table 3. All-weld metal chemical composition (wt %).**

Weld Element	MMAW-I	MMAWN-I	MMAW-II	MMAWN-II	E11018M (AWS A5.5 - 1996)
C	0.053	0.046	0.058	0.051	0.10 max
Mn	1.49	1.76	1.62	1.73	1.3 - 1.8
Si	0.58	0.46	0.60	0.40	0.60 max
S	0.02	0.02	0.019	0.018	0.03 max
P	0.025	0.028	0.024	0.028	0.03 max
Cr	0.158	0.152	0.160	0.156	0.40 max
Ni	2.31	2.45	2.23	2.47	1.25 - 2.50
Mo	0.412	0.451	0.391	0.432	0.25 - 0.50
Cu	0.021	0.027	0.025	0.023	-
Al	0.003	0.005	0.005	0.005	-
V	0.012	0.019	0.019	0.020	0.05 max
Ti	0.0023	0.0040	0.0088	0.0200	-

elements such as Mn, Ni, Mo, Ti etc. have improved in weld metal with the addition of nano size TiO<sub>2</sub> particles (sample MMAWN-I and MMAWN-II). When alloying elements are transferred from the coating (slag) to weld metal, the equilibrium is [18]

$$M_d = M_o - (M_{sl} - M_{ox}) \quad (4)$$

where  $M_d$  is the amount of alloy transferred to deposit,  $M_o$  is the initial amount of the alloy in the electrode (Core and flux coating),  $M_s$  is the remaining amount of the alloy in the slag and  $M_{ox}$  is the amount of the oxidised alloy. The unique physical properties of nano particles, resulting from quantum size and surface effects presumably enhance the recovery of the alloying elements by facilitating the slag-metal reactions. Arguments based on high reactivity of nano particles suggest that nano size TiO<sub>2</sub> would dissociate resulting in more instant generation of O<sub>2</sub> which is likely to provide more stirring effect of the weld pool. This in turn will improve slag-metal reaction. A similar behaviour was reported for nano scale marble added in a hardfacing electrode [19]. However, increasing oxygen concentration with dissociation of TiO<sub>2</sub> should increase the loss of alloying elements by oxidation. The chemical composition of weld deposit as presented in **Table 3** rather shows opposite trend except Cr which shows some loss. This observation suggests that the two potentially

competing effects would determine the final amount of alloy components transferred to the weld pool. However, considering affinity of Ti towards oxygen compared to Cr, it appears that gain of Ti can be attributed due to 1) negligible difference between the partial pressure of oxygen in the arc atmosphere and dissociation pressure of TiO<sub>2</sub> at high temperature and 2) reduction of TiO<sub>2</sub> at the boundary of metal/slag in the reaction zone of welding as per following equation:



This is not unexpected considering some loss of Si in the weld deposit with addition nano size TiO<sub>2</sub>.

### 3.2. Microstructure and Mechanical Properties of Weld Deposit

**Figure 3** shows the optical and Scanning Electron micrographs of weld deposits with and without nano size TiO<sub>2</sub>. The weld metal microstructure is affected by melting, gas dissolution, solidification and solid-state transformations. Since the weld pool region is heated to temperature as high as 2500 K, the liquid steel dissolves oxygen. The extent of oxygen dissolution depends upon the thermodynamic properties of liquid metal, gas and slag phases [20]. As the liquid weld metal cools from this temperature in the temperature range 2000°C - 1700°C,

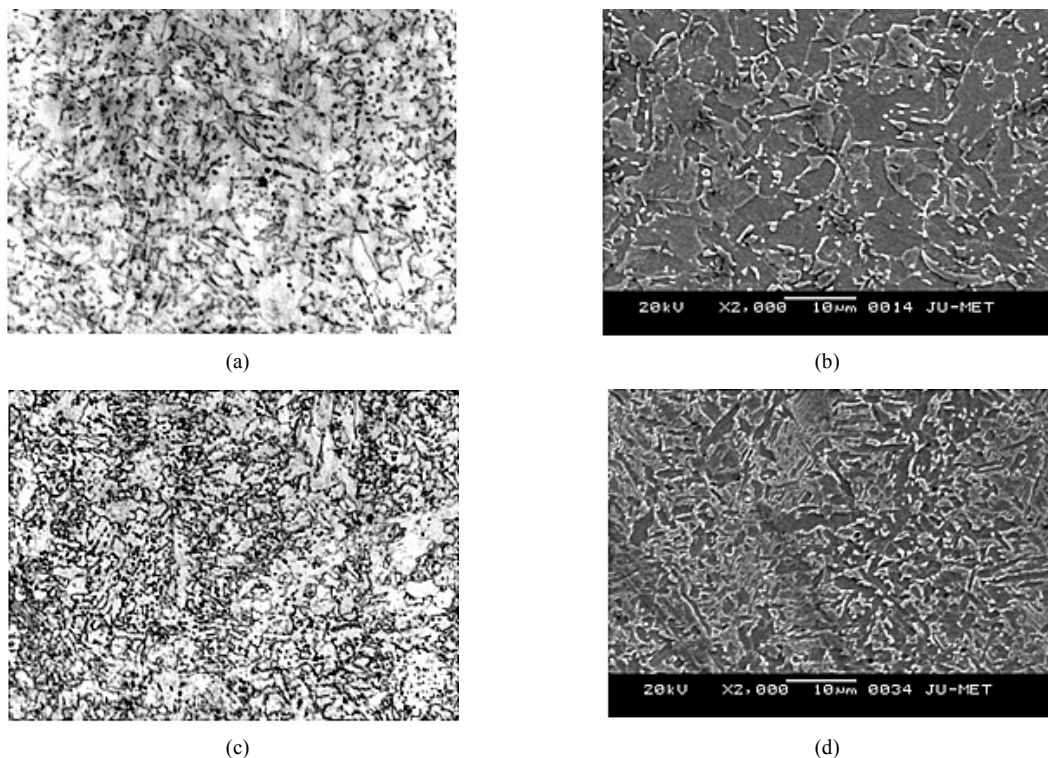


**Figure 3.** Typical microstructures of all-weld metals: (a) optical micrograph ( $\times 500$ ) & (b) SEM micrographs without nano size TiO<sub>2</sub>, (c) optical micrograph ( $\times 500$ ) and (d) SEM micrographs with nano size TiO<sub>2</sub>.

the dissolved oxygen and deoxidizing elements in the liquid steel react to form complex oxide inclusions in the range of 0.1 - 1.5  $\mu\text{m}$  size range. In the temperature range 1700°C - 1600°C, solidification to  $\delta$ -ferrite starts and envelops these oxide inclusions and this  $\delta$ -ferrite transforms to austenite. The austenite may transform to several microstructural constituents depending on chemical composition, cooling rate, and austenite grain size. In fact, the final microstructure in low carbon steel weld metals depends on complex interactions between several important variables such as inclusions, weld cooling rate and weld metal hardenability.

Although the microstructures of weld deposits as shown in **Figure 3** appear to be similar *i.e.* acicular ferrite with some bainite, considerable difference in the percentage of acicular ferrite and fineness of the structure do exists. Weld deposits with nano size TiO<sub>2</sub> addition show more acicular ferrite and more fine grained structure compared with without addition of nano size TiO<sub>2</sub>. The difference in microstructural characteristics is believed to be due to difference in chemical composition and inclusion characteristics. The inclusions in weld deposits of without nano-size TiO<sub>2</sub> particles are coarser (**Figure 4(b)**) than that of with nano-size TiO<sub>2</sub> particles which are smaller and more in number (**Figure 4(a)**). Growth and separation of oxide inclusions is influenced by factors such as number density of the nuclei, interfacial tensions and the extent of melt stirring [21]. The separation of small oxide particles in weld deposit with nano-size TiO<sub>2</sub> particles is probably favoured by the turbulent conditions existing in the hot part of the weld pool.

If there are no inclusions, acicular ferrite formation will not occur [22]. In addition, even if the inclusions are present, acicular ferrite may not form if they are ineffective. The acicular ferrite constituent, which is character-

ized by small non-aligned ferrite grains found within prior austenite grains, needs a greater degree of under cooling than primary ferrite or side plate ferrite. Furthermore, the size, type and number of weld metal inclusions, the prior austenite grain size and specific alloying additions are important considerations in achieving optimum weld metal acicular ferrite.

In a Fe-C-Mn structural steel inoculated with titanium oxide the acicular ferrite microstructure was promoted by increasing the manganese concentrations from 1.4 wt% to 2.46 wt% [23]. It was suggested that Mn segregates to austenite grain boundaries and reduces the driving force for bainite nucleation at the interface and thus facilitates the formation of acicular ferrite. Recently, He and Edmonds [24] speculated that the formation of Fe-V clusters could act as nucleation sites for acicular ferrite in addition to inclusions. Furthermore, Furahara *et al.* [25] showed that addition of V and N to C-Mn steel containing MnS inclusions led to the formation of acicular ferrite. Above discussion probably suggests that increase in hardenability elements in weld deposits with nano-size TiO<sub>2</sub> allows for greater under cooling as well as favorable inclusion characteristics for greater possibility of acicular ferrite formation.

Considering that both bainite and martensite are products of austenite, one should ascertain that high strength steel weld deposits will be free from martensite for improved strength and toughness. It is well recognized that steel will be free from martensite when the M<sub>S</sub> temperature of the steel is below its B<sub>F</sub> temperature. Interestingly, the B<sub>S</sub>, B<sub>F</sub> and B<sub>50</sub> temperatures as well as the M<sub>S</sub> and M<sub>F</sub> temperatures are all related to the chemical composition of the steel [26]. Recent constraint base model work [27] on the metallurgical criteria related with chemical composition has been used to predict the microstructure/strength of low carbon low-alloy weld deposits by the

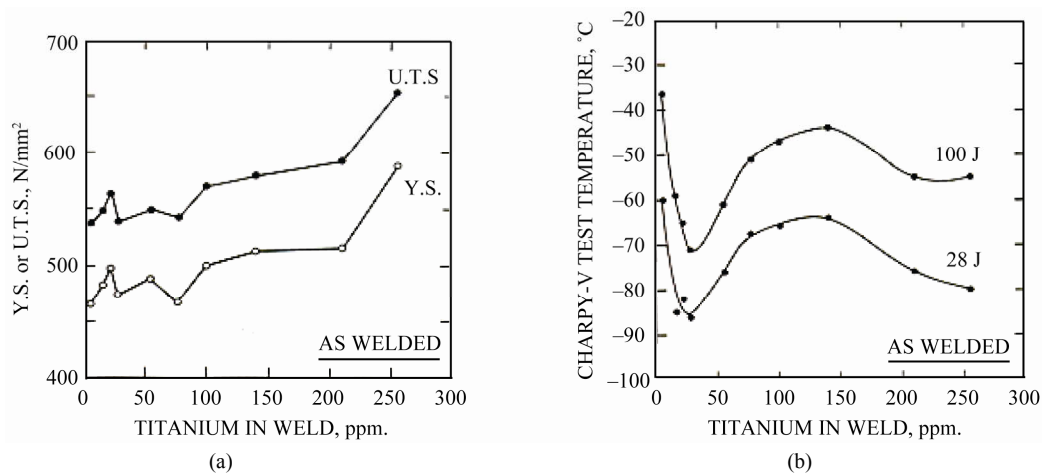


**Figure 4.** Effect of titanium on (a) YS & UTS and (b) Charpy-V-temperature.

following equations:

$$B_{50}(o_C) = 770 - (270 \times C) - (90 \times M_n) - 37(Ni) - (70 \times C_r) - 83(Mo) \quad (6)$$

$$M_s(o_C) = 561 - (474 \times C) - (33 \times Mn) - (17 \times Ni) - (21 \times Mo) \quad (7)$$

The calculated metallurgical characteristics of different weld deposits are presented in **Table 4**.

The calculated data of B<sub>50</sub> temperature as given in **Table 4** indicates the presence of bainite in all the weld deposits as the higher strength bainitic steels exhibits a B<sub>50</sub> temperature in the range of 420°C to 550°C. Furthermore, weld deposits having lower B<sub>50</sub> temperature attributes higher strength [28,29], Since bainite is a transformation product of austenite, lowering the transformation temperatures allows one to refine the grain size of the transformation product, leading to simultaneous increase in both tensile strength and ductility.

The average measured tensile and impact properties are summarized in **Table 5** for four weld deposits with and without nano size TiO<sub>2</sub>. The addition of nano size TiO<sub>2</sub> in the coating of E11018M electrode significantly elevates both YS and UTS as well as low temperature toughness. The fracture surfaces of with nano size TiO<sub>2</sub> shows quasi-cleavage mode of fracture(**Figure 5(a)**) compared to fracture surface of without nano size TiO<sub>2</sub> which exhibits almost smooth typical cleavage fracture(**Figure 5(b)**). Beside microstructural control to achieve mechanical property goal, it is necessary to control oxygen and nitrogen in the weld metal for low temperature toughness. Prior investigation using experimental flux-cored wire electrodes has shown the beneficial effect of titanium addition in controlling weld metal nitrogen content [30]. Titanium addition also served to refine the weld metal grains. Using C-Mn steel weld deposits, Evans [31] determined that there are two optimum

**Table 4. Calculated metallurgical characteristics of different weld deposits.**

Weld sample	B <sub>50</sub> Temperature (°C)	M <sub>s</sub> Temperature (°C)
MMAW-I	491	439
MMAWN-I	460	430
MMAW-II	479	434
MMAWN-II	463	428

**Table 5. Mechanical properties of different weld deposits.**

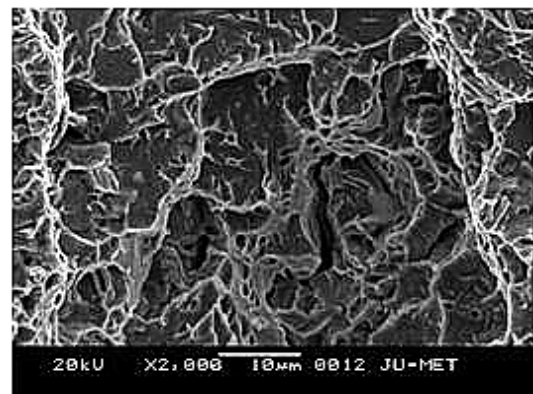
Weld deposits	YS (MPa)	UTS (MPa)	% Elongation	Charpy Impact toughness at -51°C (J)
MNAW-I	690	765	23	28
MMAWN-I	710	791	24	33
MMAW-II	701	770	22	29
MMAWN-II	734	823	25	35

titanium concentration regarding impact toughness e.g. 30 and 200 ppm as shown schematically in **Figure 5(b)**. Also both YS and UTS increased with increase in Ti content in the weld metal (**Figure 5(a)**). Evans [32] also reported a complex interaction between Mn and Ti. The optimum impact toughness occurred at 35 ppm Ti and 1.4 pct. Mn. The effect of Ti was more pronounced at higher level of Mn. Titanium therefore acts as deoxidizer, grain refiner and nitrogen getter and at the same time it is very sensitive to the performance of weld deposits. The beneficial effect of Ti on mechanical properties of weld deposits, toughness in particular, at some critical concentration is supported in the present study. Thus, to enhance the performance of weld deposits particularly the toughness, it is very important to control the amount of Ti in weld deposits.

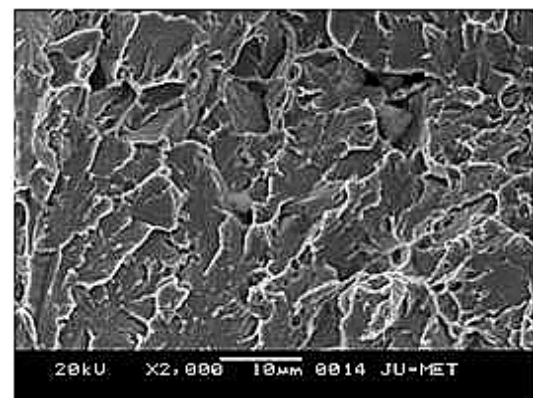
#### 4. Conclusions

The following conclusions may be drawn from the study:

- 1) The introduction of nano size TiO<sub>2</sub> in the coating of coated electrode (E11018M) improved recovery of elements such as Mn, Ni, Mo, Ti etc.



(a)



(b)

**Figure 5. SEM fractographs (a) weld metal with nano size TiO<sub>2</sub> and (b) weld metal without nano size TiO<sub>2</sub>.**

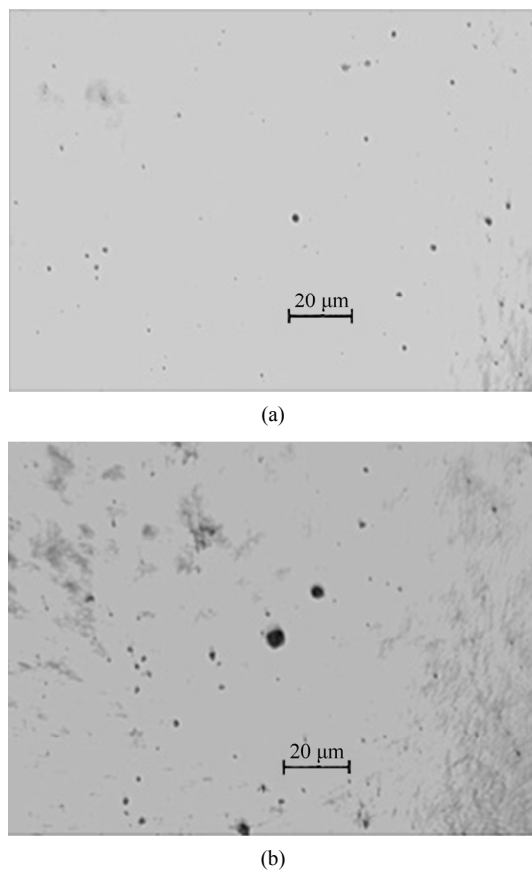


**Figure 6. Optical micrographs showing inclusions: (a) weld metal with nano size TiO<sub>2</sub> and (b) weld metal without nano size TiO<sub>2</sub>.**

2) A significant influence on microstructure and mechanical properties of weld deposits has been observed with addition of nano size TiO<sub>2</sub>. Both strength and toughness at -51°C of weld deposits with nano size TiO<sub>2</sub> increased compared to without nano size TiO<sub>2</sub>.

3) In order to enhance the performance of weld deposits particularly the toughness, it is very important to control the amount of Ti in weld deposits.

## REFERENCES

- [1] L. E. Svensson, "Consumable for Welding High Strength Steels," *Svetsaren*, Vol. 54, No. 1-2, 1999, pp. 29-33.
- [2] M. George, J. Still and P. Terry, "Gas Metal Arc Welds for High Toughness Applications-Microstructure and Other Factors," *Metal Construction*, Vol. 13, No. 12, 1981, pp. 730-737.
- [3] T. Keeler, "Innershield Welding Part 1-Development and Applications," *Metal Construction*, Vol. 13, No. 11, 1981, pp. 667-673.
- [4] D. J. Widgery, L. Karlsson, M. Muruganath and E. Keehan, "Approaches to the Development of High-Strength Weld Metals," *Proceedings of 2nd International Symposium on High Strength Steel*, Stikklestad, Verdal, Norway: European Coal and Steel Community (ECSC), B-1049 Brussels, Belgium, 2002.
- [5] W. C. Leslie, "The Physical Metallurgy of Steels," McGraw-Hill, London, 1981.
- [6] L. E. Svensson, "Control of Microstructure and Properties in Steel Arc Welds," CRC Press, Inc., 1994.
- [7] G. M. Evans and N. Bailey, "Metallurgy of Basic Weld Metal," Abington Publishing, 1997. doi:10.1533/9781845698850
- [8] M. Nakanishi, *Journal of the Japan Welding Society*, Vol. 50, 1981, p. 5.
- [9] J. A. Gianetto, *et al.*, *Welding Journal*, Vol. 71, 1992, p. 407-S.
- [10] S. Liu and D. L. Olson, "The Role of Non-metallic Inclusions in Controlling HSLA Weld Microstructures," *Welding Journal*, Vol. 65, 1986, p.134-s-149-s.
- [11] I. Watanabe and T. Kojima, *Journal of the Japan Welding Society*, Vol. 49, 1980, p. 772 N. Mori: IIW Doc. IX – 1158-1180.
- [12] N. Mori, H. Homma, S. Ohkita and M. Wakabayashi, "Mechanisms of Notch Toughness Improvement in Ti-B Bearing Weld Metal," IIW Doc. IX-1196-81.
- [13] N. Christensen and J. Chipman, "Slag-Metal Interaction in Arc Welding," *Welding Research Council, Bulletin*, Vol. 15, January 1953, pp. 1-14.
- [14] U. Mitra and T. W. Eagar, "Slag-Metal Reaction during Submerged Arc Welding of Alloy Steels," *Metallurgical and Materials Transactions A*, Vol. 15A, 1984, pp. 217-227. doi:10.1007/BF02644404
- [15] G. R. Bolton, T. J. Moore and E. S. Tankins, "Slag-Metal Reactions in Submerged Arc Welding," *Welding Journal*, Vol. 42, No. 7, 1963, pp. 289-s-297-s.
- [16] M. C. Flemings, "Solidification Processing," McGraw-Hill, New York, 1974.
- [17] R. H. Forst, D. L. Olson and S. Liu, "Influence of Solidification on Inclusion Formation in Welds," *Proceedings of the 3rd International Conference on Trends in Welding Research*, ASM International, Gatlinburg, Tennessee, 1992.
- [18] W. Y. Zhang, "Welding Metallurgy," Mechanical Engineering Press, Beijing, 2003.
- [19] B. Chen, F. Han, Y. Huang, K. Lu, Y. Liu and L. Li, "Influence of Nanoscale Marble (Calcium Carbonate CaCO<sub>3</sub>) on Properties of D600 R Surfacing Electrode," *Welding Journal*, Vol. 88, March 2009, pp. 99-s-103-s.
- [20] S. A. David and T. Deb Ray, "Current Issues and Problems in Welding Science," *Science*, Vol. 257, 1992, pp. 497-502. doi:10.1126/science.257.5069.497
- [21] U. Lindborg and K. Torsell, *Transactions on TMS-AIME*, Vol. 242, 1968, pp. 94-102.
- [22] J.S. Byun, J.H. Shim and Y. W. Cho, "Influence of Mn on Microstructure Evolution in Ti-Killed C-Mn Steel," *Scripta Materialia*, Vol. 48, No. 4, 2003, pp. 449-454. doi:10.1016/S1359-6462(02)00437-2

- [23] S. K. Liu and J. Zhang, "The Influence of the Si and Mn Concentrations on the Kinetics of the Bainite Transformation in Fe-C-Si-Mn Alloys," *Metallurgical and Materials Transactions A*, Vol. 21, No. 6, 1990, pp. 1517-1525.
- [24] K. He and D. V. Edmonds, "Formation of Acicular Ferrite and Influence of Vanadium Alloying," *Materials Science and Technology*, Vol. 18, 2002, pp. 289-296.  
[doi:10.1179/026708301225000743](https://doi.org/10.1179/026708301225000743)
- [25] T. Furuhashi, J. Yamaguchi, N. Sugita, N. Miyamoto and T. Maki, "Nucleation of Proeutectoid Ferrite on Complex Precipitates in Austenite," *ISIJ International*, Vol. 43, No. 10, 2003, pp. 1630-1639.  
[doi:10.2355/isijinternational.43.1630](https://doi.org/10.2355/isijinternational.43.1630)
- [26] W. Steven and A. G. Haynes, "The Temperature of Formation of Martensite and Bainite in Low-Alloy Steels," *Journal of the Iron and Steel Institute*, Vol. 183, No. 8, 1956, pp. 349-359
- [27] K. Sampath, "Constraints-Based Modeling Enables Successful Development of a Welding Electrode Specification for Critical Navy Applications," *Welding Journal*, August 2005, pp. 131-s-138-s.
- [28] K. J. Irvine and F. B. Pickering, "Low-Carbon Bainitic Steels," *Journal of the Iron and Steel Institute*, Vol. 184, No. 12, 1957, pp. 292-309.
- [29] W. C. Leslie, "The Physical Metallurgy of Steels," McGraw-Hill International Book Company, London, 1981, pp. 201-205.
- [30] R. J. Wrong and M. D. Hayes, "The Metallurgy, Welding and Qualification of Microalloyed (HSLA) Steel Weldments," AWS, Miami, 1990, pp. 450-489.
- [31] G. M. Evans, "Factors Affecting the Microstructure and Properties of C-Mn All-Weld Metal Deposits," *Welding Research Abroad*, Vol. 28, No. 1, 1983, pp. 1-69.
- [32] G. M. Evans, "The Effect of Titanium on the Microstructure and Properties of C-Mn All-Weld Metal Deposits," *OERLIKON-Schweibmitt*, Vol. 49, No. 125, 1991, pp. 22-33.